Published in final edited form as:
J Cereb Blood Flow Metab. 2005 October ; 25(10): 1265–1279. doi:10.1038/sj.jcbfm.9600132.

Functional, perfusion and diffusion MRI of acute focal ischemic brain injury

Qiang Shen[1], **Hongxia Ren**[1], **Haiying Cheng**[1], **Marc Fisher**[2], and **Timothy Q Duong**[1]

[1]Department of Neurology, Yerkes Primate Research Center, Emory University, Atlanta, Georgia, USA

[2]Department of Neurology, University of Massachusetts Medical School, Worcester, Massachusetts, USA

Abstract

Combined functional, perfusion and diffusion magnetic resonance imaging (MRI) with a temporal resolution of 30 mins was performed on permanent and transient focal ischemic brain injury in rats during the acute phase. The apparent diffusion coefficient (ADC), baseline cerebral blood flow (CBF), and functional MRI (fMRI) blood-oxygen-level-dependent (BOLD), CBF, and $CMRO_2$ responses associated with CO_2 challenge and forepaw stimulation were measured. An automated cluster analysis of ADC and CBF data was used to track the spatial and temporal progression of different tissue types (e.g., normal, 'at risk,' and ischemic core) on a pixel-by-pixel basis. With permanent ischemia (n = 11), forepaw stimulation fMRI response in the primary somatosensory cortices was lost, although vascular coupling (CO_2 response) was intact in some animals. Control experiments in which the right common carotid artery was ligated without causing a stroke (n = 8) showed that the delayed transit time had negligible effect on the fMRI responses in the primary somatosensory cortices. With temporary (15-mins, n = 8) ischemia, transient CBF and/or ADC declines were observed after reperfusion. However, no T_2 or TTC lesions were observed at 24 h except in two animals, which showed very small subcortical lesions. Vascular coupling and forepaw fMRI response also remained intact. Finally, comparison of the relative and absolute fMRI signal changes suggest caution when interpreting *percent* changes in disease states in which the baseline signals are physiologically altered; quantitative CBF fMRI are more appropriate measures. This approach provides valuable information regarding ischemic tissue viability, vascular coupling, and functional integrity associated with ischemic injury and could have potential clinical applications.

Keywords

BOLD; CBF; $CMRO_2$; DWI; fMRI; ISODATA; penumbra; perfusion–diffusion mismatch; PWI

Introduction

Diffusion-weighted (DWI) and perfusion-weighted (PWI) magnetic resonance imaging (MRI) techniques offer the potential to noninvasively classify 'normal', 'at-risk,' and 'ischemic' tissues associated with stroke during the acute phase. Brain tissues with perfusion deficits below a critical threshold (Hossmann, 1994) experience metabolic energy failure, membrane depolarization, and subsequent cellular swelling. These changes precipitate a reduction in the apparent diffusion coefficient (ADC) of brain water and are manifested as hyperintense regions

Correspondence: Dr TQ Duong, Department of Neurology, Yerkes National Primate Research Center, Emory University, 954 Gatewood Road NE, Atlanta, GA 30329, USA. tduong@emory.edu.

on DWI (Moseley *et al*, 1990). During the acute phase, the DWI abnormality is initially smaller relative to the area of perfusion deficit. As ischemia evolves, most of this DWI abnormality expands and eventually coincides with the abnormal PWI area. The difference in the abnormal region defined by the PWI and DWI in acute stroke is commonly referred to as the 'perfusion–diffusion' mismatch. It has been suggested that the 'perfusion–diffusion' mismatch is potentially salvageable and approximates the '*ischemic penumbra*' (Astrup *et al*, 1981).

With the advent of functional MRI (fMRI), it becomes possible to assess the integrity of vascular coupling and neural function of 'at-risk' and 'salvaged' tissues, as defined by DWI and PWI. Anatomically defined 'at-risk' and salvaged tissues may or may not show functional deficit and thus fMRI adds a unique and important measure to stroke imaging. The most widely used fMRI technique is based on the blood-oxygen-level-dependent (BOLD) signal (Ogawa *et al*, 1990) and the cerebral blood flow (CBF) signal. The BOLD contrast originates from intravoxel magnetic field inhomogeneity induced by paramagnetic deoxyhemoglobin in the red blood cells. Changes in regional deoxyhemoglobin content can be visualized in susceptibility-sensitized (i.e., T_2^*-weighted) BOLD images. The BOLD fMRI is based on a principle discovered over 100 years ago (Roy and Sherrington, 1890) that neuronal activity is intricately coupled to CBF. When a task is performed, regional CBF increases disproportionally, which can be measured using the arterial-spin labeling MRI technique. The CBF increase overcompensates the stimulus-evoked increase in oxygen consumption needed to fuel the elevated neural activity, resulting in a regional reduction in deoxyhemoglobin concentration. Thus, the CBF and BOLD fMRI signals increase during stimulus-evoked changes in neural activity relative to basal conditions, making it possible to dynamically and noninvasively map changes in brain functions.

Furthermore, Davis *et al* introduced an eloquent formalism based on the BOLD biophysical model (Ogawa *et al*, 1993) to estimate stimulus-evoked $CMRO_2$ changes based on BOLD and CBF (or cerebral blood volume (CBV)) measurements. The advantage of Davis' formalism over existing formalisms is that there are no *a priori* assumptions regarding resting capillary or venous oxygen saturation, blood volume fraction, blood flow, and metabolic rate of oxygen. All these parameters and other physiologic quantities are lumped into the constant *M*, which can be measured on a pixel-by-pixel basis using a calibration procedure involving CO_2 challenge. Although this $CMRO_2$ model has yet to be validated, especially in ischemic injury, estimates of stimulus-evoked $CMRO_2$ changes in stroke could yield interesting and valuable information regarding tissue metabolism.

The use of fMRI to evaluate functional status requires preservation of the hemodynamic and metabolic coupling. Carbon dioxide, a potent vasodilator, plays an important role in modulating blood flow associated with increased neuronal activity. The hypercapnia model in which CO_2 is added to the breathing gas has been widely used to examine the vascular coupling (Weiss *et al*, 1983; Ueki *et al*, 1988; Kim and Ugurbil, 1997; Davis *et al*, 1998; Hoge *et al*, 1999; Corfield *et al*, 2001; Duong *et al*, 2001). One major advantage of hypercapnic challenge is that it increases blood flow, and thus the BOLD signal, of the entire brain without changing neural activity or metabolism, thereby making possible the evaluation of vascular coupling without the added effects of metabolic changes. Previous studies on blood flow regulation after prolonged ischemia suggest that CO_2 reactivity is severely disturbed after ischemic injury (Schmidt-Kastner *et al*, 1986; Ueki *et al*, 1988).

While a few fMRI studies on stroke patients have been reported (Pineiro *et al*, 2002; Guadagno *et al*, 2003; Binkofski and Seitz, 2004), similar studies in animal stroke models have been limited. Animal models where focal ischemia can be reproducibly studied under controlled conditions are important for systemically evaluating the integrity of vascular coupling and functional status of 'at risk' and salvaged tissues defined by perfusion and diffusion imaging.

Functional MRI using an exogenous CBV contrast agent (MION) and BOLD contrast have recently been applied to study stroke rats during the *chronic* phase to evaluate functional reorganization (Dijkhuizen *et al*, 2001, 2003). Functional MRI assessment of the dynamically evolving ischemic tissue during acute stroke, however, have not been reported, likely because of the stringent need for high spatiotemporal resolution and the lack of a suitable animal model. Most of stroke studies in rats used chloral hydrate as the anesthetic (Li *et al*, 1999, 2000; Shen *et al*, 2003) whereas essentially all forepaw-stimulation fMRI studies in normal rats use α-chloralose (Mandeville *et al*, 1998; Silva *et al*, 1999; Duong *et al*, 2000). α-Chloralose became a popular anesthetic for fMRI studies in rats because it can induce nonresponsiveness without depressing the central nervous system to the same extent as many other common anesthetics. However, animals recovering from α-chloralose anesthesia exhibit atypical behavior (Lees, 1972) and thus α-chloralose is only approved for terminal studies. In addition, fMRI studies under α-chloralose typically require mechanical ventilation with repeated blood-gas sampling to optimize the fMRI responses and it is relatively difficult to maintain a constant level of anesthesia with injectable anesthetics in general (Austin *et al*, 2005) for eliciting consistent fMRI responses from the onset (i.e., during acute ischemia) and throughout the studies. More recently, a robust forepaw stimulation model in rats was showed under isoflurane anesthesia and spontaneously breathing conditions where the animals can maintain their own physiology throughout the experiment without the need for repeated blood-gas sampling (Liu *et al*, 2004a). This model could be well suited for repeated fMRI studies of acute and chronic stroke in a longitudinal fashion.

In this study, we developed and applied a combined diffusion, perfusion, and functional MRI protocol to study focal cerebral ischemia during the acute phase with a 30-mins temporal resolution and reasonable spatial resolution. Quantitative perfusion and diffusion imaging was performed and an improved ISODATA clustering technique (Shen *et al*, 2004) was used to classify normal, ischemic core, and 'diffusion–perfusion mismatch' tissues based on ADC and CBF characteristics. Blood-oxygen-level-dependent, CBF, and $CMRO_2$ fMRI associated with hypercapnic challenge and forepaw stimulation were used to evaluate the integrity of vascular coupling and neural function, respectively, as ischemia progressed during the acute phase. Blood-oxygen-level-dependent, CBF, and $CMRO_2$ fMRI responses in different ISODATA-derived ischemic tissue types and in the forepaw somatosensory cortices of the right ischemic hemisphere (RH) were analyzed and compared with the homologous regions in the normal left hemisphere (LH). This approach was tested in the permanent and transient (15-mins) acute focal brain ischemia in rats under isoflurane, breathing spontaneously.

Materials and methods

Animal Preparation

Twenty seven male Sprague–Dawley rats (300 to 350 g, Taconic Farms, NY, USA) were anesthetized with 2% isoflurane in air during surgery. Three groups of animals were studied: (i) permanent focal brain ischemia of the RH was induced with intraluminal middle cerebral artery occlusion (MCAO) (n = 11, Group I), (ii) transient (15-mins) focal brain ischemia (n = 8, Group II) was induced using the same method and reperfusion was performed outside the magnet, and (iii) the right common carotid artery (CCA) was ligated but without causing a stroke to evaluate the possible effect of delayed transit time on the fMRI responses (n = 8, Group III). Measurements were made before and during CCA ligation in the same animals where the CCA occlusion was achieved remotely while the animals were in the magnet. The left femoral artery was catheterized for blood-gas sampling and physiologic monitoring. Once the rats were secured in an MR-compatible rat stereotaxic headset, anesthesia was reduced to 1.1% to 1.2% isoflurane. Rats breathed spontaneously without mechanical ventilation. Rectal temperature was maintained at 37.0°C ± 0.5°C. Heart rate (HR) and mean arterial blood

pressure (MABP) via the arterial line were recorded continuously onto a PC via the Biopac system (Santa Barbara, CA, USA). Respiration rate (RR) was derived from the slow modulations on top of the cardiac waveforms. Blood gas was typically sampled once during a break between imaging trials. All recorded physiologic parameters were within normal physiologic ranges. Magnetic resonance imaging data were acquired at 30, 90, and 180 mins and again at 24 h after ischemia.

Hypercapnic Challenge and Forepaw Stimulation

Hypercapnic challenges used a premixed gas of 10% CO_2 with 21% O_2 and balance N_2. Forepaw somatosensory stimulation used the previously optimized parameters under identical isoflurane anesthetic condition in normal animals (Liu *et al*, 2004a): 6 mA current with 0.3 ms pulse duration at 3 Hz. These stimulation parameters did not cause an increase in MABP. Needle electrodes were inserted under the skin of the two forepaws before surgery. The electrodes were connected in series and the two forepaws were stimulated simultaneously. During each time point (30-mins imaging block), one trial of hypercapnic challenge and two trials of forepaw stimulation were presented with a 4-mins break (without imaging) between trials. Each trial consisted of 4 mins of data acquired during baseline and 2 mins of data acquired during hypercapnic challenge or forepaw stimulation.

MR Experiments

Magnetic resonance imaging experiments were performed on a 4.7-T/40-cm magnet, a Biospec Bruker console (Billerica, MA, USA), and a 20-G/cm gradient insert (ID = 12 cm, 120-μs rise time). A surface coil (2.3-cm ID) was used for brain imaging and a neck coil (Silva *et al*, 1999; Duong *et al*, 2000) for perfusion labeling. Coil-to-coil electromagnetic interaction was actively decoupled. A complete imaging block lasted 30 mins where ADC, basal CBF, hypercapnic, and forepaw-stimulation fMRI were acquired.

ADC_{av} was obtained by averaging three ADC maps with diffusion-sensitive gradients separately applied along the *x*, *y* or *z* direction. Single shot, echo-planar images (EPI) were acquired with matrix = 64 × 64, spectral width = 200 kHz, TR = 2 secs (90° flip angle), TE = 37.5 ms, b = 4 and 1,170 secs/mm^2, Δ = 24 ms, δ = 4.75 ms, FOV = 2.56 cm × 2.56 cm, eight 1.5-mm slices, and 16 averages (total time ~2.5 mins).

Combined CBF and BOLD measurements were made using the continuous arterial spin-labeling technique with single-shot, gradient-echo, EPI acquisition. Paired images were acquired alternately—one with arterial spin labeling and the other without (control). MR parameters were as follows: data matrix = 64 × 64, FOV = 2.56 cm × 2.56 cm, eight 1.5-mm slices, TE = 20 ms, and TR = 2 secs (90° flip angle). Continuous arterial spin labeling employed a 1.78-s square radiofrequency pulse to the labeling coil in the presence of 1.0 G/cm gradient along the flow direction such that the condition of adiabatic inversion was satisfied. The sign of the frequency offset was switched for control (nonlabeled) images. For each set of CBF and BOLD measurements, 60 pairs of images (4 mins) were acquired during baseline and 30 pairs (2 mins) during hypercapnic challenge or forepaw stimulation.

Data Analysis

Data analysis used codes written in Matlab (MathWorks Inc., Natick, MA, USA) and the STIMULATE (University of Minnesota) software. Coregistration of images obtained during the acute phase and at 24 h used an in-house software, which involved both manual and automatic alignment without spatial interpolation, as described previously (Liu *et al*, 2004a).

Calculation of basal ADC and CBF maps—Apparent diffusion coefficient maps with intensity in unit of mm^2/sec were calculated pixel-by-pixel by using (Stejskal and Tanner,

1965), $ADC = -\ln(S_1/S_0)/(b_1-b_0)$ where $b_i=\gamma^2 G_i^2\delta^2(\Delta - \delta/3)$, where ln is the natural logarithm, S_0 and S_1 are the signal intensities obtained with b_0 and b_1, respectively. The *b*-value is proportional to the gradient strength (G), magnetogyric ratio (γ), duration of each gradient pulse (δ), and the time (Δ) between applications of the two gradient pulses. Apparent diffusion coefficient maps were calculated at each time point.

Cerebral blood flow images (S_{CBF}) with intensity in units of mL/g/min were calculated (Silva *et al*, 1999; Duong *et al*, 2000) pixel-by-pixel using, $S_{CBF} = \lambda/T_1(S_C-S_L)/(S_L + (2\alpha-1)\ S_C)$, where S_C and S_L are signal intensities of the control and labeled images, respectively, and λ is the partition coefficient and α is the labeling efficiency. Basal CBF images were obtained from the baseline period (without stimulation) of all three trials of the fMRI measurements within each time point.

ISODATA analysis of diffusion and perfusion images—An improved ISODATA clustering algorithm was used to statistically resolve and identify tissues as 'normal', 'mismatch' and 'ischemic core' based on tissue ADC and CBF characteristics as described elsewhere (Shen *et al*, 2004). Only five anterior slices were analyzed to avoid susceptibility distortion around the ear canals associated with the posterior slices. ROIs of the whole brain were carefully drawn to avoid the edge of the brain-skull interface based on CBF maps with reference to ADC maps. Pixels with ADC higher than 1.0×10^{-3} mm^2/sec (i.e., CSF pixels) and the corpus callosum were excluded from analysis. Clustering for ADC and baseline CBF was performed individually at each time point for each animal. Three clusters were resolved: (1) pixels with normal ADC and baseline CBF were assigned to be 'normal' tissue, (2) pixels with low ADC and baseline CBF were assigned to be 'ischemic core', and (3) pixels with normal ADC but low baseline CBF were assigned to be 'perfusion–diffusion mismatch'.

Functional MRI responses in different ISODATA clusters were analyzed. Scatterplots of CBF versus ADC and BOLD versus ADC under baseline and stimulated (CO_2 or forepaw) conditions were generated at each time point. Different ISODATA clusters were color-coded on the scatterplots.

Evolution of 'mismatch' pixels—The temporal and spatial evolution of the 'mismatch' pixels, defined at 30 mins after occlusion, was evaluated as they migrated to different clusters. Apparent diffusion coefficient, CBF, and BOLD under baseline and stimulated (CO_2 or forepaw) conditions were analyzed for the pixels that subsequently migrated into the normal zone, core zone, or remained in the mismatch zone at 180-mins after ischemia. For permanent occlusion, ischemia stopped evolving 180 mins after occlusion, which was taken as the imaging end point as shown previously (Shen *et al*, 2003; Meng *et al*, 2004).

Calculation of M and $CMRO_2$ changes—$CMRO_2$ was calculated using (Davis *et al*, 1998),

$$\frac{\Delta BOLD}{BOLD_0} = M\left(1 - \left(\frac{CMR_{O_2}}{CMR_{O_2}|_0}\right)^{\beta}\left(\frac{CBF}{CBF_0}\right)^{\alpha-\beta}\right) \quad (1)$$

where M is the proportionality constant and parameters with subscript zero indicate baseline values. Grubb's factor (α) of 0.38 (Grubb *et al*, 1974; Mandeville *et al*, 1999) and β of 1.5 (Boxerman *et al*, 1995; Davis *et al*, 1998) were taken to be constants, reflecting the effects of blood volume and deoxyhemoglobin concentration on the BOLD signal, respectively. M values were calculated from the hypercapnia (CBF and BOLD) data using the same equation where

the $CMRO_2/CMRO_2|_0$ was set to unity because brief and mild hypercapnia does not alter $CMRO_2$ (Kety and Schmidt, 1948; Novack *et al*, 1953). Stimulus-evoked $CMRO_2$ changes from an ROI of the primary somatosensory cortex were derived from the stimulus-evoked BOLD and CBF time courses associated with forepaw stimulation. Additional details of the model including error propagation have been described elsewhere (Liu *et al*, 2004a).

Hypercapnic responses in different tissue types—Images obtained during the transition period between baseline and stimulus onset (30 secs for CO_2 challenge and 15 secs for forepaw stimulation) were discarded. Blood-oxygen-level-dependent images were obtained from the control (nonlabeled) images of the CBF measurements. Blood-oxygen-level-dependent and CBF magnitude and percent changes relative to baselines were calculated: (1) on a pixel-by-pixel basis, (2) for the ISODATA-derived normal, mismatch, and core clusters, and (3) for the ROI of the forepaw somatosensory cortices.

Forepaw-stimulation responses in the forepaw cortices—Cross correlation analysis associated with the forepaw primary somatosensory cortices was performed. ROI of the normal LH forepaw cortices were drawn based on the averaged cross correlation activation maps of all time points with references to the rat brain atlas and MRI anatomical images to avoid bias to any particular time point. The forepaw ROIs on the ischemic RH were obtained by symmetrically reflecting the LH ROIs along the midline to the RH. Apparent diffusion coefficient, baseline CBF, and fMRI signals in the forepaw primary somatosensory cortex ROI were analyzed pixel-by-pixel as well as by averaging pixels within the forepaw ROI. Magnitude baseline CBF and CBF changes were computed. Baseline T_2^*-weighted signal intensities (within the forepaw ROI) of the ischemic RH was normalized with respect to the homologous ROI of the LH for comparison.

All data values in text are expressed as mean ± s.d. and in graphs as mean ± s.e.m. A *P*-value <0.05 (*t*-test) was taken to be statistically significant.

Results

Permanent Occlusion (Group I): CO_2 Responses in Different ISODATA-Derived Clusters

Images and maps at 30 mins after ischemia of one representative animal subjected to permanent focal ischemia are shown in Figure 1A. Basal CBF images depict a large perfusion deficit and ADC images depict a smaller ADC lesion in the ischemic RH. Nine out of 11 rats showed a substantial and evolving ‘perfusion–diffusion’ mismatch and a few of these animals showed some persistent mismatch at 180 mins. The forepaw primary somatosensory cortices typically showed an evolving a perfusion–diffusion mismatch because of its anatomical location close to the anterior communicating artery. The two remaining animals showed large infarcts at the onset without apparent mismatch at 30 mins. ISODATA analysis yielded three distinct tissue types in the RH, namely, normal (blue pixels), mismatch (green pixels), and core (red pixels). The fMRI maps showed that the hypercapnic challenge evoked a marked CBF increases in the LH, slightly attenuated CBF increases in the RH ‘normal’ tissues and essentially no evoked CBF increases in the RH ischemic ‘core’ and ‘mismatch’ tissues. Hypercapnia-induced CBF increases were essentially absent in regions with perfusion deficit. Interestingly, although dependent on the precise threshold used, the BOLD activated areas appeared to be larger than the CBF activation areas, suggesting differences in metabolic and CBF changes associated with ischemic injury.

The ADC and CBF values of different ISODATA-derived clusters are summarized in Table 1. LH ADC and LH basal CBF were similar at all time points. In the normal zone of the ischemic

RH, ADC and CBF were normal. In the mismatch zone, ADC was marginally reduced but CBF was significant reduced. In the core zone, both ADC and CBF were markedly reduced.

Pixel-by-pixel scatterplot analysis of CBF versus ADC under baseline and CO_2 challenge from one animal is shown in Figure 1B (left panel). The LH basal CBF was 1.2 ± 0.7 mL/g/min (whole brain average). Hypercapnia markedly increased CBF, with 90% of all pixels showing a pixel-by-pixel ΔCBF increase ranging from 0.5 to 3 mL/g/min. In the RH, the normal, mismatch and core clusters were derived using the ISODATA analysis and color coded. Essentially all 'core' and 'mismatch' pixels showed no CO_2-induced CBF increases. Most of the RH 'normal' pixels showed significant CO_2-induced CBF increases but were smaller in magnitude relative the LH.

The scatterplot analysis of BOLD versus ADC is shown on the right panel of Figure 1B. The wide distribution of the normalized baseline T_2^*-weighted signal intensities in the LH is indicative of tissue heterogeneity, tissue physiologic status (i.e., hypoxia), and nonuniform signal intensity profile of the surface coil. Nonetheless, in the LH, the CO_2-induced BOLD increases were evident. Although the RH 'core' pixels showed lower baseline T_2^*-weighted signal intensities because of hypoxia-induced increase in deoxyhemoglobin concentration and/or changes in blood volume, different ISODATA clusters (derived via ADC and baseline CBF data) were not well segregated based on T_2^*-weighted signal intensities. CO_2-induced ΔBOLD versus *ADC* showed slightly better cluster separation visually but nonetheless were significantly less resolved compared with the corresponding CO_2-induced ΔCBF versus *ADC*. The average BOLD fMRI responses were 3.5%, 3.3%, 1.1%, and −0.8% in the normal LH, normal RH, mismatch, and core clusters, respectively.

The group-average hypercapnia-induced CBF and BOLD changes in the LH and in different RH ISODATA clusters at different time points are summarized in Figure 1C. For permanent occlusion, ischemia stopped evolving 180 min after occlusion (Shen *et al*, 2003; Meng *et al*, 2004), which was taken as the imaging end point. Baseline CBF of the RH normal cluster was similar to that of the LH. However, the RH CO_2-induced CBF and BOLD fMRI responses, although robust, were attenuated relative to the LH fMRI responses. There were trends of improvements in the RH fMRI responses over time. Baseline CBF of the RH mismatch and ischemic core were markedly reduced and their CO_2-induced fMRI responses were essentially absent. BOLD responses in the RH mismatch and ischemic core were also markedly attenuated. Note that only BOLD percent changes were plotted because baseline T_2^*-weighted intensities could not be compared across different brain regions because of tissue heterogeneity and nonuniform intensity profile of the surface coil.

Tracking the Perfusion–Diffusion Mismatch

To better understand the tissue at risk, mismatch pixels were tracked as ischemia progressed. The mismatch pixels at 30 min were taken as references and individual pixels were dynamically tracked in terms of their basal CBF, CBF, and BOLD fMRI responses as they migrated to different zones at 180 min (Figure 1D). Majority of the mismatch pixels migrated to the 'ischemic core' at 180 min after ischemia, consistent with the definition of ischemic penumbra. Pixels that migrated to the core zone at 180 min after ischemia showed ADC decreases (0.67 ± 0.03 at 30 min to 0.48 ± 0.02 at 180 min); those that remained in the mismatch zone or those that migrated to the normal zone showed no ADC decreases relative to the normal LH. As expected, pixels migrating to the 'normal' zone showed a slightly higher baseline CBF, ΔCBF, and ΔBOLD responses at 30 min and significantly higher baseline CBF, ΔCBF, and BOLD responses at 180 min. In contrast, pixels that remained in the mismatch zone or migrated to the ischemic 'core' zone showed lower baseline CBF, ΔCBF, and ΔBOLD responses at both 30 and 180 min. Although the magnitudes of the RH CO_2-induced ΔCBF were markedly reduced,

the CO_2-induced CBF percent changes, notably, were significant and comparable with those of the normal LH because of division by the small RH baseline values under ischemia. This observation suggests caution in interpreting relative percent changes in disease state.

Permanent Occlusion (Group I): CO_2 and Forepaw Responses in the Primary Somatosensory Cortices

In addition to analyzing the CO_2 response profiles of different ISODATA-derived tissue types, functional integrity associated with forepaw stimulation in ischemic brain injury was also evaluated. CBF versus ADC and BOLD versus ADC scatterplots of pixels within the forepaw somatosensory cortices associated with hypercapnic challenge and forepaw stimulation are showed in Figure 2A. In the normal LH, CO_2 challenge and forepaw stimulation evoked significant changes in the CBF and BOLD fMRI responses (red pixels) relative to the baseline (green pixels), with the stimulus-evoked CBF increases showing significantly larger dynamic ranges. In the ischemic RH, the center of mass of pixels associated with CO_2 challenge showed small but observable CBF and BOLD increases. Stimulus-evoked changes in the center of mass of these pixels in the ischemic RH were, however, visually negligible.

Hypercapnic responses within the primary somatosensory cortices are summarized in Figure 2B (top panel). In the normal LH across all time points, baseline CBF in the forepaw somatosensory cortex was ~1.05 mL/g/min, CO_2 inhalation increased CBF to ~3 mL/g/min, and forepaw stimulation increased CBF to ~1.4 mL/g/min. In the ischemic RH, baseline CBF in the forepaw somatosensory cortex was 0.25 mL/g/min, CO_2 challenge induced a small CBF increase of <0.2 mL/g/min. However, if the data were expressed as percent changes, CO_2-induced CBF increases were 50 to 70%, again suggesting caution in interpreting relative percent changes in physiologically perturbed state. Baseline T_2^*-weighted signal intensities of the RH were normalized with respective to those of the normal LH forepaw cortex for comparison. Assuming that the signal drop off within the small forepaw primary somatosensory area due to the surface coil application was negligible, baseline normalized T_2^*-weighted signal intensities between the LH and RH could be compared. Under basal condition without stimulation, normalized baseline T_2^*-weighted image intensities in the ischemic RH were slightly reduced by 2.5% as expected because of hypoxia and/or blood volume changes, as reported previously (Roussel *et al*, 1995; van der Toorn *et al*, 1995). In the normal LH, CO_2 challenge increased BOLD by ~7.4% whereas, in the ischemic RH, CO_2 challenge increased BOLD by 2.5%. This is in marked contrast to the magnitude stimulus-evoked CBF responses that was negligible in the ischemic RH. This difference between BOLD and CBF responses associated with forepaw stimulation is consistent with that associated with CO_2 challenge (Figure 1B).

The forepaw stimulation responses within the primary somatosensory cortices are shown in Figure 2B (bottom panel). Baseline CBF, baseline T_2^*-weighted signal intensities, and fMRI responses did not vary substantially across different time points after ischemia. In the normal LH, forepaw evoked robust BOLD and CBF responses. In the ischemic RH, forepaw stimulation evoked a negligible CBF increase. However, BOLD increase was not negligible. This difference between BOLD and CBF responses associated with forepaw stimulation is consistent with that associated with CO_2 challenge (Figures 1A and 2B top panel), suggesting uncoupling of metabolic activity and blood flow.

To better understand the potential uncoupling of metabolism and CBF, stimulus-evoked $CMRO_2$ changes associated with forepaw stimulation in permanent ischemic brain injury were also estimated. Table 2 summarizes the *M* values and stimulus-evoked $CMRO_2$ changes in the primary somatosensory cortices in the LH and RH at different time points after occlusion. *M* is the proportionality constant in the $CMRO_2$ model and it reflects the hemodynamic coupling.

M value in the normal LH was ~10% across different time points whereas that in the ischemic RH was reduced by half, ca. ~5%. Forepaw-stimulation-induced $CMRO_2$ increase was ~10% in the LH and ~3% in the RH.

Transient (15-mins) Occlusion (Group II)

Images and maps at 30 mins after ischemia of one representative animal subjected to transient (15-mins) focal ischemia are shown in Figure 3A. All eight animals exhibited regions of hypoperfusion at the first imaging time point (~30 mins) but only one animal showed detectable ADC reduction at 30 mins. Six animals showed heterogeneous and mild hypoperfusion at 180 mins, but no ADC lesions were observed. Six animals showed no T_2 or TTC lesions at 24 h after ischemia and two showed very small T_2 and TTC abnormality (43 mm^3) at 24 h in the subcortical region. CBF images at 24 h were normal with no apparent hypo- or hyper-perfusion. Hypercapnic challenge evoked marked CBF and BOLD increases in both LH and RH and there were no statistical differences in CO_2-induced fMRI responses between the LH and RH at all time points ($P > 0.05$). *Basal* CBF and *basal* T_2^*-weighted signal intensities were not statistically different between the LH and RH somatosensory cortices ($P > 0.05$). Similarly, there were also no statistical differences in the *stimulus-evoked* CBF and BOLD fMRI responses between the LH and RH somatosensory cortices ($P > 0.05$).

Stimulus-evoked $CMRO_2$ changes and *M* values in the LH and RH primary somatosensory cortices after transient ischemic brain injury were estimated (Table 3). *M* values were not statistically different between LH and RH primary somatosensory cortices ($P > 0.05$) and they ranged from 7.7% to 9.4% across different time points. Forepaw-stimulation-induced $CMRO_2$ increases in the LH and RH were also not statistically different between LH and RH primary somatosensory cortices ($P > 0.05$) and they ranged from 13% to 21% across different time points.

Effects of Mean Transit Time on fMRI Responses: CCA Occlusion Without Causing Stroke (Group III)

Attenuation of the fMRI responses could be because of ischemia and/or delayed mean transit time associated with occlusion of major arteries. To investigate the potential effects of delayed mean transit time on the fMRI responses, control fMRI experiments were performed in which the common carotid artery was clipped (occluded) remotely but without causing a stroke as confirmed by ADC measurements (data not shown). Functional MRI responses obtained from the primary somatosensory cortices are summarized in Figure 4. Although both the baseline and stimulus-evoked CBF under the *clip* condition were marginally lower relative to the *no-clip* condition, there were no statistical differences between *clip* and *no-clip* data ($P > 0.05$). Subcortical structures, however, showed significantly delayed MTT effect. The effective whole-brain CBF values were reduced by 20%.

Discussion

The major results of this study are: (1) Combined diffusion, perfusion, and fMRI of ischemic brain injury during the acute phase was performed with a temporal resolution of 30 mins. (2) Automated ISODATA cluster analysis of MR tissue characteristics (ADC, CBF, and fMRI responses) was implemented, making it possible to spatially and temporally track different tissue types on pixel-by-pixel basis, providing valuable information regarding tissue viability, vascular coupling, and functional integrity associated with the dynamic evolution of ischemic brain injury. (3) Permanent cerebral ischemia resulted in a complete loss of neuronal activity in the primary somatosensory cortices in all animals whereas vascular coupling was intact in some animals. Loss of vascular coupling and/or functional integrity preceded ADC lesion and were temporally associated with the perfusion decline. Thus, fMRI could potentially serve as

an earlier and complementary indictor for risk of ischemic brain injury. (4) Transient (15-mins) cerebral ischemia exhibited transient CBF and/or ADC decline. However, no permanent injury was observed in essentially all animals at 3 and 24 h. Vascular coupling and fMRI responses in the forepaw cortices were also normal. (5) The effect of delayed transit time on the fMRI responses in the primary somatosensory cortices due to occlusion of major arteries in this stroke model was negligible. (6) Cerebral blood flow fMRI responses appeared to have larger dynamic ranges than the BOLD responses and pixel-by-pixel CBF changes were more apparent, suggesting a potentially better mapping signal. (7) Finally, caution must be exercised when interpreting relative fMRI signal changes in physiologically perturbed states in which the baseline signals are altered, resulting in erroneous percent changes. Measurements of magnitude changes (such as quantitative CBF changes) might be necessary to provide accurate measures of increased neural activity under physiologically perturbed conditions.

Errors in CBF Measurements

Although consistent with many established techniques, the accuracy of this CBF technique could be subject to errors from magnetization-transfer (Silva *et al*, 1995), transit-time (Calamante *et al*, 1996; Zhou *et al*, 2001), and water-exchange (Silva *et al*, 1997; Zhou *et al*, 2001; Parkes and Tofts, 2002) effects. The magnetization-transfer effect was not an issue with the actively decoupled two-coil system (Duong *et al*, 2000; Silva *et al*, 2000). Transit-time effect in small animals and water-exchange effect are small (Silva *et al*, 1997; Zhou *et al*, 2001; Parkes and Tofts, 2002) and unlikely to alter the conclusions of this study. Ischemia-induced changes in transit time, however, could result in significant errors and remains to be vigorously validated. In the control experiments in which the CCA was occluded, it was estimated that the upper limit of CBF error was ~20% (whole brain). Despite the potential error associated with delayed transit time in stroke, quantitative CBF fMRI arguably is a better measure considering the alternative fMRI percent changes, which incorrectly reflect neural activity because of the marked changes in baseline values under ischemic conditions.

Advantages and Disadvantages of Forepaw Stimulation fMRI of Acute Stroke Under Isoflurane Anesthesia

Forepaw stimulation is a good model for assessing the functional integrity in the rat stroke model herein because the *primary somatosensory cortices* generally experience an evolving perfusion–diffusion mismatch, most of which will inevitably become infarcted if left untreated. Although widely used in fMRI studies of normal animals, α-chloralose is less suited for fMRI studies of both acute and chronic ischemic brain injury. In this study, we chose to use isoflurane under spontaneously breathing condition which has been previously optimized to yield robust responses (Liu *et al*, 2004a). As this study shows, fMRI studies could be performed during the acute and chronic phase of ischemic brain injury.

The disadvantage is that isoflurane is a potent vasodilator and a strong neural suppressant, which could attenuate the hemodynamic and neural responses, respectively. Nonetheless, robust fMRI responses could be detected as shown herein and previously in normal animals (Liu *et al*, 2004a; Sicard and Duong, 2005). Isoflurane has also been suggested to have some neuroprotective effects (Mortier *et al*, 2000; Elsersy *et al*, 2004). Our unpublished data showed that the infarct sizes under isoflurane with *permanent focal ischemia* were not statistically different from that under chloral hydrate, whereas the infarct size under isoflurane with *transient focal ischemia* was smaller, depending on experimental conditions. Nonetheless, the choice of isoflurane anesthetic should not affect the overall conclusion of this study, namely, that these MRI techniques and the animal model offer a unique means to dynamically study the vascular coupling and functional integrity of different ischemic tissue types as a function of ischemic evolution in both acute and chronic phase.

Magnitude versus Percent Changes

A striking observation is that although the magnitudes of the CO_2-induced ΔCBF in the ischemic RH were markedly reduced, the CO_2-induced CBF percent changes were substantial and comparable with those of the normal LH (Figure 2B). This is because of the division by small RH baseline values associated with ischemia. Comparison of the magnitude and percent change suggests that cautions must be exercised when interpreting fMRI data based on fMRI percent changes in disease states where the baseline physiology is markedly altered. We further suggest that measurements of magnitude changes are needed for fMRI studies under perturbed conditions. Similar observations were reported associated with fMRI associated with systemic cocaine administration which caused substantial transient changes in mean arterial blood pressure, heart rate and respiration (Liu *et al*, 2004b). These physiologic effects on stimulus-evoked fMRI responses had been systemically evaluated in another study (Sicard and Duong, 2005) in which the relative and quantitative CBF, normalized (with respect to a fixed baseline) BOLD and $CMRO_2$ fMRI changes associated with forepaw stimulation in normal animals were measured where the baseline conditions were physiologically modulated by changing the inhaled CO_2 or O_2 gas concentrations. It was found that quantitative CBF, normalized $CMRO_2$ and BOLD signals are accurate indicators of increased neural activity under mild physiologic perturbation whereas relative fMRI signal changes are not.

Differences in Hypercapnic and Functional Responses

In some animals, there was persistent mismatch at 180 mins and the RH forepaw somatosensory cortex did not show ADC lesions at 180 mins and 24 h. It was also noted that the RH forepaw somatosensory cortices did respond to CO_2 challenge but did not respond to forepaw stimulation (Figures 1A and 2B) in some animals. One potential explanation is that the RH forepaw somatosensory cortex was functional silence because of the systemic ischemic shock although the RH forepaw somatosensory cortex was not injured. The other potential explanation is that the functional connection from which the cortex receives its inputs (i.e., thalamus) was severed, although both vascular coupling and functions of the RH forepaw somatosensory cortex were intact. As such, no forepaw-stimulation fMRI responses in the RH somatosensory cortices were detected despite their normal ADC and CO_2 fMRI responses. This notion is supported by the extended subcortical injury but remains to be validated.

Differences between CBF and BOLD fMRI Responses

In the ischemic RH, the CO_2 BOLD activated areas were larger than the CO_2 CBF activated areas (Figure 1A) and the CO_2 and forepaw BOLD responses were attenuated less than the CO_2 and forepaw CBF responses (Figure 2B). This observation suggests uncoupling of metabolism, CBV and/or CBF associated with ischemia. For example, $CMRO_2$ could be reduced, leading to a larger BOLD increase. There is evident that basal CBV elevates in ischemic injury (Roussel *et al*, 1995; van der Toorn *et al*, 1995), which could modulate the BOLD percent changes. It should be noted that activated areas in Figure 1B are dependent on the precise thresholds used. Because the BOLD and CBF contrast-to-noise ratios were different, different thresholds were used which could potentially lead to bias. In Figure 1B, thresholds in the CO_2 challenge studies were judicially set for display such that the central ischemic core showed no activated pixels. In Figure 2B, however, ROI analysis of the primary forepaw somatosensory cortices was performed without using thresholds and thus there was no bias. In brief, the differences between CBF and BOLD fMRI responses are likely genuine, indicative of metabolic and hemodynamic uncoupling associated with ischemic brain injury.

Imaging $CMRO_2$ in Acute Stroke

To further investigate the apparent metabolic and hemodynamic uncoupling, we attempted, as a first step, to estimate $CMRO_2$ changes associated with ischemic brain injury. The *M* values

in the normal LH (10% and 8% in the permanent and transient ischemic model, respectively) were higher than that (ca., 5%) reported previously with a shorter TE of 15 ms in normal rats under essentially identical preparation (Liu *et al*, 2004a). This difference was expected because a shorter TE yields a smaller *M* value (see equation(1)). Nonetheless, this difference does not affect the $CMRO_2$ determination as long as the same MR parameters were used in both the *M* and $CMRO_2$ measurements in a single setting. Forepaw-stimulation-induced $CMRO_2$ increases in the normal LH (10% and 17% in the permanent and transient ischemic model, respectively) were smaller than that of the 24% ± 6% increase in normal animals reported previously (Liu *et al*, 2004a). We have no explanation for this discrepancy. A potential explanation for the apparent discrepancy in stimulation-induced $CMRO_2$ changes between the previous and current study could be that the stroke surgery *per se* could cause a reduced stimulus-evoked $CMRO_2$ change even in the unaffected LH. $CMRO_2$ estimates showed that metabolism was markedly reduced in both mismatch and core tissues.

Magnetic resonance imaging-based $CMRO_2$ model remains to be validated. Davis' $CMRO_2$ model has not been previously used in disease states. Although the stimulus-evoked $CMRO_2$ changes and the *M* values in the ischemic regions herein were reasonable and consistent, the Davis' $CMRO_2$ model may not be valid under physiologically perturbed states. Direct validation of this MRI-based $CMRO_2$ technique under normal and disease states is difficult because of a lack of gold standard for *in vivo* $CMRO_2$ measurement. Cross correlation with microPET-$CMRO_2$ techniques would provide further support of this valuable MRI-based $CMRO_2$ technique. Nonetheless, estimates of $CMRO_2$ changes in stroke using this model, particularly in the ‘perfusion–diffusion mismatch’ where the coupling could remain largely intact, yielded interesting and valuable information regarding tissue metabolism and the underlying vascular coupling.

Conclusion

The MRI protocol and data analysis approach showed herein offer a useful means to characterize acute and chronic ischemic brain injury with respect to anatomical, physiologic and functional status at reasonably high spatiotemporal resolution. Future studies will make use of this approach, along with immunohistological and behavioral assessment, to systemically study ischemic brain injury with variable functional outcomes (i.e., by increasing the transient ischemic duration) and where reperfusion will be performed while the animals are in the magnet to obtain a preocclusion data set for robust pixel-by-pixel analysis. This approach has the potential to be translated into clinical settings.

Acknowledgments

This work was supported in part by the NIH (NINDS, R01-NS45879) and the American Heart Association (SDG-0430020N).

References

Astrup J, Symon L, Siesjo BK. Thresholds in cerebral ischemia: the ischemic penumbra. Stroke 1981;12:723–5. [PubMed: 6272455]

Austin VC, Blamire AM, Allers KA, Sharp T, Styles P, Matthews PM, Sibson NR. Confounding effects of anesthesia on functional activation in rodent brain: a study of halothane and a-chloralose anesthesia. NeuroImage 2005;24:92–100. [PubMed: 15588600]

Binkofski F, Seitz RJ. Modulation of the BOLD-response in early recovery from sensorimotor stroke. Neurology 2004;63:1223–9. [PubMed: 15477542]

Boxerman JL, Hamberg LM, Rosen BR, Weisskoff RM. MR contrast due to intravascular magnetic susceptibility perturbations. Magn Reson Med 1995;34:555–66. [PubMed: 8524024]

Calamante F, Williams SR, van Bruggen N, Kwong KK, Turner R. A model for quantification of perfusion in pulsed labeling techniques. NMR Biomed 1996;9:79–83. [PubMed: 8887372]

Corfield DR, Murphy K, Josephs O, Adams L, Turner R. Does hypercapnia-induced cerebral vasodilation modulate the hemodynamic response to neural activation? Neuroimage 2001;13:1207–11. [PubMed: 11352626]

Davis TL, Kwong KK, Weisskoff RM, Rosen BR. Calibrated functional MRI: mapping the dynamics of oxidative metabolism. Proc Natl Acad Sci USA 1998;95:1834–9. [PubMed: 9465103]

Dijkhuizen RM, Ren J, Mandeville JB, Wu O, Ozdag FM, Moskowitz MA, Rosen BR, Finklestein SP. Functional magnetic resonance imaging of reorganization in rat brain after stroke. Proc Natl Acad Sci USA 2001;98:12766–71. [PubMed: 11606760]

Dijkhuizen RM, Singhal AB, Mandeville JB, Wu O, Halpern EF, Finklestein SP, Rosen BR, Lo EH. Correlation between brain reorganization, ischemic damage, and neurologic status after transient focal cerebral ischemia in rats: a functional magnetic resonance imaging study. J Neurosci 2003;23:510–7. [PubMed: 12533611]

Duong TQ, Iadacola C, Kim SG. Effect of hyperoxia, hypercapnia and hypoxia on cerebral interstitial oxygen tension and cerebral blood flow in the rat brain: an 19F/1H study. Magn Reson Med 2001;45:61–70. [PubMed: 11146487]

Duong TQ, Silva AC, Lee SP, Kim SG. Functional MRI of calcium-dependent synaptic activity: cross correlation with CBF and BOLD measurements. Magn Reson Med 2000;43:383–92. [PubMed: 10725881]

Elsersy H, Sheng H, Lynch JR, Moldovan M, Pearlstein RD, Warner DS. Effects of isoflurane versus fentanyl-nitrous oxide anesthesia on long-term outcome from severe forebrain ischemia in the rat. Anesthesiology 2004;100:1160–6. [PubMed: 15114213]

Grubb RL, Raichle ME, Eichling JO, Ter-Pogossian MM. The effects of changes in $PaCO_2$ on cerebral blood volume, blood flow, and vascular mean transit time. Stroke 1974;5:630–9. [PubMed: 4472361]

Guadagno JV, Calautti C, Baron JC. Progress in imaging stroke: emerging clinical applications. Br Med Bull 2003;65:145–57. [PubMed: 12697622]

Hoge RD, Atkinson J, Gill B, Crelier GR, Marrett S, Pike GB. Investigation of BOLD signal dependence on cerebral blood flow and oxygen consumption: the deoxyhemoglobin dilution model. Magn Reson Med 1999;42:849–63. [PubMed: 10542343]

Hossmann KA. Viability thresholds and the penumbra of focal ischemia. Ann Neurol 1994;36:557–65. [PubMed: 7944288]

Kety SS, Schmidt CF. The effects of altered arterial tensions of carbon dioxide and oxygen on cerebral blood flow and cerebral oxygen consumption of normal young men. J Clin Invest 1948;27:484–91.

Kim SG, Ugurbil K. Comparison of blood oxygenation and cerebral blood flow effects in fMRI: estimation of relative oxygen consumption change. Magn Reson Med 1997;38:59–65. [PubMed: 9211380]

Lees P. Pharmacology and toxicology of alpha chloralose: a review. Vet Rec 1972;91:330–3. [PubMed: 4562133]

Li F, Han SS, Tatlisumak T, Liu KF, Garcia JH, Sotak CH, Fisher M. Reversal of acute apparent diffusion coefficient abnormalities and delayed neuronal death following transient focal cerebral ischemia in rats. Ann Neurol 1999;46:333–42. [PubMed: 10482264]

Li F, Silva MD, Sotak CH, Fisher M. Temporal evolution of ischemic injury evaluated with diffusion-, perfusion-, and T_2-weighted MRI. Neurology 2000;54:689–96. [PubMed: 10680805]

Liu ZM, Schmidt KF, Sicard KM, Duong TQ. Imaging oxygen consumption in forepaw somatosensory stimulation in rats under isoflurane anesthesia. Magn Reson Med 2004a;52:277–85. [PubMed: 15282809]

Liu ZM, Shen Q, Sicard KM, Febo M, Ferris CF, Stein EA, Duong TQ. Imaging cocaine-induced changes in BOLD, CBF and oxygen consumption. Proc Int Soc Magn Reson Med 2004b;1:278.

Mandeville JB, Marota JJ, Ayata C, Moskowitz MA, Weisskoff RM, Rosen BR. MRI measurement of the temporal evolution of relative CMRO2 during rat forepaw stimulation. Magn Reson Med 1999;42:944–51. [PubMed: 10542354]

Mandeville JB, Marota JJ, Kosofsky BE, Keltner JR, Weissleder R, Rosen BR, Weisskoff RM. Dynamic functional imaging of relative cerebral blood volume during rat forepaw stimulation. Magn Reson Med 1998;39:615–24. [PubMed: 9543424]

Meng X, Fisher M, Shen Q, Sotak CH, Duong TQ. Characterizing the diffusion/perfusion mismatch in experimental focal cerebral ischemia. Ann Neurol 2004;55:207–12. [PubMed: 14755724]

Mortier E, Struys M, Herregods L. Therapeutic coma or neuroprotection by anaesthetics. Acta Neurol Belg 2000;100:225–8. [PubMed: 11233677]

Moseley ME, Cohen Y, Mintorovitch J, Chileuitt L, Shimizu H, Kucharczyk J, Wendland MF, Weinstein PR. Early detection of regional cerebral ischemia in cats: comparison of diffusion- and T2-weighted MRI and spectroscopy. Magn Reson Med 1990;14:330–46. [PubMed: 2345513]

Novack P, Shenkin H, Bortin L, Goluboff B, Soffe AM. The effects of carbon dioxide inhalation upon the cerebral blood flow and cerebral oxygen consumption in vascular disease. J Clin Invest 1953;32:696–702. [PubMed: 13069617]

Ogawa S, Lee TM, Kay AR, Tank DW. Brain magnetic resonance imaging with contrast dependent on blood oxygenation. Proc Natl Acad Sci USA 1990;87:9868–72. [PubMed: 2124706]

Ogawa S, Menon RS, Tank DW, Kim SG, Merkle H, Ellermann JM, Ugurbil K. Functional brain mapping by blood oxygenation level-dependent contrast magnetic resonance imaging. Biophys J 1993;64:800–12.

Parkes LM, Tofts PS. Improved accuracy of human cerebral blood perfusion measurements using arterial spin labeling: accounting for capillary water permeability. Magn Reson Med 2002;48:27–41. [PubMed: 12111929]

Pineiro R, Pendlebury S, Johansen-Berg H, Matthews PM. Altered hemodynamic responses in patients after subcortical stroke measured by functional MRI. Stroke 2002;33:103–9. [PubMed: 11779897]

Roussel SA, van Bruggen N, King MD, Gadian DG. Identification of collaterally perfused areas following focal cerebral ischemia in the rat by comparison of gradient echo and diffusion-weighted MRI. J Cereb Blood Flow Metab 1995;15:578–86. [PubMed: 7790407]

Roy CS, Sherrington CS. On the regulation of blood supply of the brain. J Physiol 1890;1:85–108.

Schmidt-Kastner R, Grosse Ophoff B, Hossman KA. Delayed recovery of CO_2 reactivity after one hour's complete ischaemia of cat brain. J Neurol 1986;233:367–9. [PubMed: 3100726]

Shen Q, Meng X, Fisher M, Sotak CH, Duong TQ. Pixel-by-pixel spatiotemporal progression of focal ischemia derived using quantitative perfusion and diffusion imaging. J Cereb Blood Flow Metab 2003;23:1479–88. [PubMed: 14663344]

Shen Q, Ren H, Bouley J, Fisher M, Duong TQ. Dynamic tracking of acute ischemic tissue fates using improved unsupervised ISODATA analysis of high-resolution quantitative perfusion and diffusion data. J Cereb Blood Flow Metab 2004;24:887–97. [PubMed: 15362719]

Sicard KM, Duong TQ. Effects of hypoxia, hyperoxia and hypercapnia on baseline and stimulus-evoked BOLD, CBF and $CMRO_2$ in spontaneously breathing animals. NeuroImage 2005;25:850–8. [PubMed: 15808985]

Silva A, Williams D, Koretsky A. Evidence for the exchange of arterial spin-labeled water with tissue water in rat brain from diffusion-sensitized measurements of perfusion. Magn Reson Med 1997;38:232–7. [PubMed: 9256102]

Silva AC, Lee SP, Iadecola C, Kim SG. Early temporal characteristics of CBF and deoxyhemoglobin changes during somatosensory stimulation. J Cereb Blood Flow Metab 2000;20:201–6. [PubMed: 10616809]

Silva AC, Lee SP, Yang C, Iadecola C, Kim SG. Simultaneous blood oxygenation level-dependent and cerebral blood flow functional magnetic resonance imaging during forepaw stimulation in the rat. J Cereb Blood Flow Metab 1999;19:871–9. [PubMed: 10458594]

Silva AC, Zhang W, Williams DS, Koretsky AP. Multi-slice MRI of rat brain perfusion during amphetamine stimulation using arterial spin labeling. Magn Reson Med 1995;33:209–14. [PubMed: 7707911]

Stejskal EO, Tanner JE. Spin diffusion measurements: spin echoes in the presence of a time-dependent field gradient. J Chem Phys 1965;42:288–92.

Ueki M, Linn F, Hossmann KA. Functional activation of cerebral blood flow and metabolism before and after global ischemia of rat brain. J Cereb Blood Flow Metab 1988;8:486–94. [PubMed: 3392113]

van der Toorn A, Dijkhuizen RM, Tulleken CA, Nicolay K. T1 and T2 relaxation times of the major 1H-containing metabolites in rat brain after focal ischemia. NMR Biomed 1995;8:245–52. [PubMed: 8732180]

Weiss HR, Buchweitz E, Sinha AK. Effect of hypoxic-hypercapnia on cerebral regional oxygen consumption and supply. Circ Res 1983;51:494–503. [PubMed: 7127684]

Zhou J, Wilson DA, Ulatowski JA, Traystman RJ, van Zijl PC. Two-compartment exchange model for perfusion quantification using arterial spin tagging. J Cereb Blood Flow Metab 2001;21:440–55. [PubMed: 11323530]

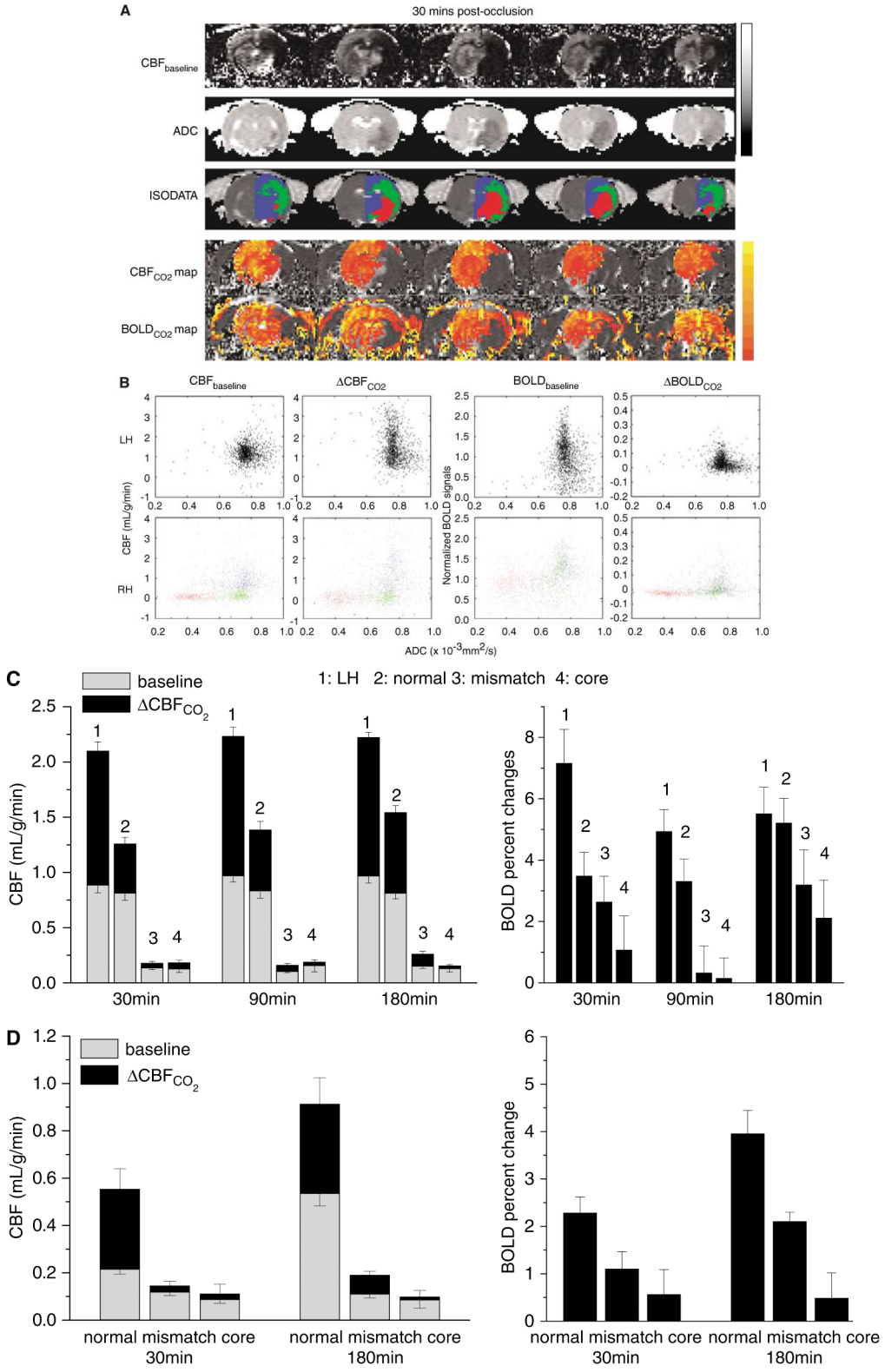

Figure 1.

Permanent occlusion—CO_2 functional magnetic resonance imaging (fMRI) responses in different ISODATA-derived clusters (n = 11). (**A**) Representative CBF and apparent diffusion coefficient (ADC) maps, ISODATA clusters overlaid on ADC maps, ΔCBF_{CO_2} and $\Delta BOLD_{CO_2}$ percent change maps overlaid on CBF images of a rat subjected to permanent focal ischemia at the 30-min time point. ISODATA cluster analysis yielded 'normal' (blue), 'perfusion–diffusion mismatch' (green), and 'ischemic core' (red) clusters. Gray-scale bar indicates ADC ranging from 0 to 0.001 mm^2/sec and CBF 0 to 3 mL/g/min. Color bar indicates ΔCBF ranging from 10% to 400% and ΔBOLD 1% to 10%. (**B**) Scatterplots of baseline CBF versus ADC, ΔCBF_{CO_2} versus *ADC*, normalized baseline T_2^*-weighted signal intensities versus ADC, and $\Delta BOLD_{CO_2}$ versus *ADC* for the left hemisphere (LH) and the right hemisphere (RH) at 30 mins after ischemia (one animal). ISODATA-derived clusters were assigned as 'normal' (blue), 'perfusion–diffusion mismatch' (green) and 'ischemic core' clusters (red). (**C**) Group-average baseline CBF, ΔCBF_{CO_2}, and $\Delta BOLD_{CO_2}$ of the normal left hemisphere and the ISODATA-derived normal, mismatch, core clusters of the right ischemic hemisphere at three time points after ischemia. (**D**) Temporal evolution of the group-average baseline CBF, ΔCBF_{CO_2}, and $\Delta BOLD_{CO_2}$ of the 'mismatch' before and after migration to different zones as ischemia progressed. Mismatch at 30 mins after ischemia was used as the reference and these mismatch pixels were tracked as they migrated to different zones at 180 mins after ischemia.

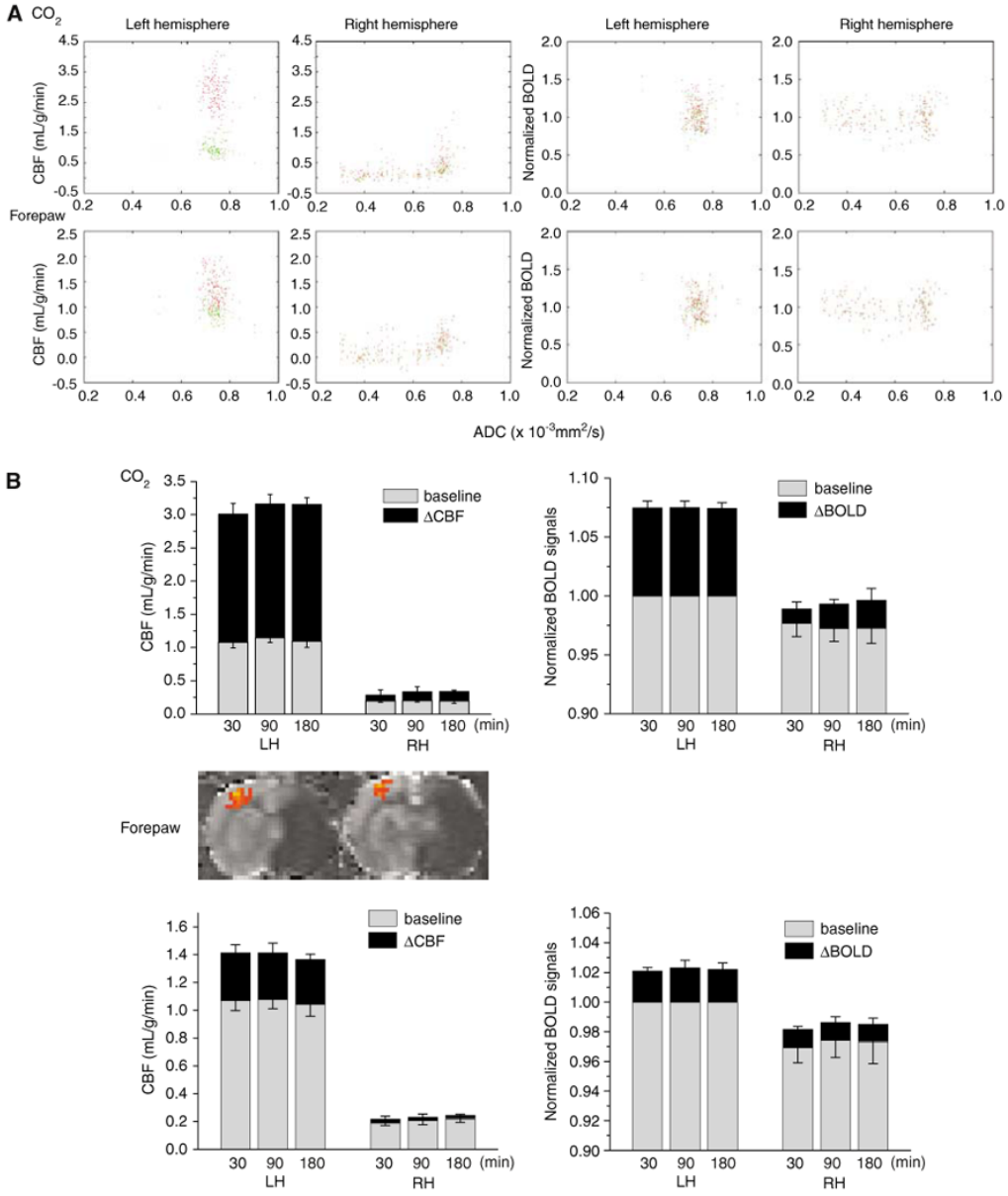

Figure 2.

Permanent occlusion—CO_2 and forepaw functional magnetic resonance imaging (fMRI) responses in the primary somatosensory cortices (n = 11). (**A**) Group-average scatterplots of baseline CBF versus apparent diffusion coefficient (ADC), ΔCBF_{CO_2} versus *ADC*, normalized baseline T_2^*-weighted signal intensities versus ADC, and $\Delta BOLD_{CO_2}$ versus *ADC* for the left hemisphere and the right hemisphere (RH) at 180 mins after ischemia. Data were obtained from the forepaw somatosensory cortices. The green pixels are baseline conditions and red pixels are stimulus-evoked changes. (**B**) Group-average fMRI responses to CO_2 challenge and forepaw stimulation in the forepaw somatosensory cortices. Baseline CBF and ΔCBF fMRI responses, normalized T_2^*-weighted signal intensities and ΔBOLD fMRI responses are shown for different time points after ischemia. The inset shows representative CBF fMRI activation maps of forepaw stimulation.

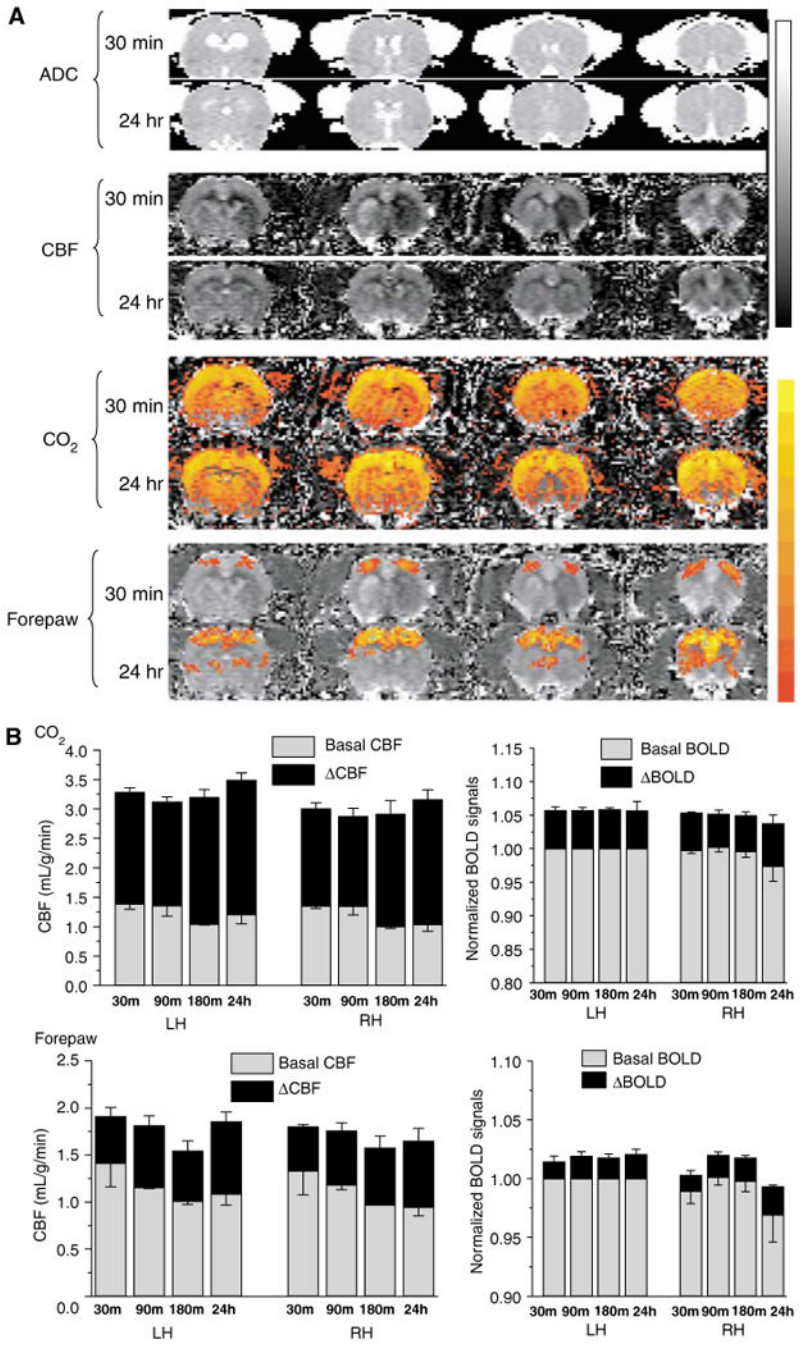

Figure 3.

Transient occlusion–CO_2 and forepaw functional magnetic resonance imaging (fMRI) responses in the primary somatosensory cortices (n = 8). (**A**) Apparent diffusion coefficient (ADC) maps, baseline CBF, ΔCBF_{CO_2}, and forepaw stimulation ΔCBF of a rat subjected to transient ischemia. Gray-scale bar indicates ADC ranging from 0 to 0.001 mm^2/sec and CBF 0 to 3 mL/g/min. Color bar indicates ΔCBF ranging from 10% to 400% and ΔBOLD 1% to 10%. (**B**) Group-average baseline CBF, ΔCBF_{CO_2}, and $\Delta BOLD_{CO_2}$ of the normal left hemisphere (LH) and the right hemisphere (Rh) ISODATA-derived normal, mismatch, core clusters of the right ischemic hemisphere.

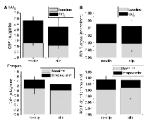

Figure 4.

Common carotid artery occlusion without causing stroke—CO_2 and forepaw functional magnetic resonance imaging (fMRI) responses in the primary forepaw somatosensory cortices (n = 8). (**A**) Group-average baseline CBF and ΔCBF associated with CO_2 challenge and forepaw stimulation. (**B**) Group-average normalized BOLD and ΔBOLD associated with CO_2 challenge and forepaw stimulation.

Table 1

Group average ADC and CBF for different time point and different area (*n* = 11, mean ± s.d.)

	ADC (× 10^{-3} mm^2/sec)			CBF baseline (mL/g/min)		
	30 min	**90 min**	**180 min**	**30 min**	**90 min**	**180 min**
LH	0.75 ± 0.02	0.76 ± 0.01	0.75 ± 0.01	0.89 ± 0.21	0.97 ± 0.17	0.97 ± 0.20
Normal	0.74 ± 0.02	0.74 ± 0.02	0.74 ± 0.03	0.81 ± 0.20	0.83 ± 0.20	0.81 ± 0.15
Mismatch	0.69 ± 0.02	0.70 ± 0.02	0.70 ± 0.03	0.13 ± 0.04	0.10 ± 0.03	0.15 ± 0.06
Core	0.51 ± 0.02	0.48 ± 0.02	0.46 ± 0.03	0.13 ± 0.12	0.15 ± 0.20	0.13 ± 0.11

ADC, apparent diffusion coefficient; CBF, cerebral blood flow; LH, left hemisphere.

Table 2

Permanent occlusion: group-average percent *M* and $CMRO_2$ from the primary forepaw somatosensory cortices (*n* = 11, mean ± s.d.)

	LH	RH
M (%)		
30 mins	11.0 ± 2.0	7.3 ± 2.1
90 mins	10.9 ± 2.1	7.1 ± 3.1
180 mins	10.6 ± 2.1	7.0 ± 2.4
$\Delta CMRO_2$ *(%)*		
30 mins	9.6 ± 3.5	3.4 ± 2.3
90 mins	10.9 ± 3.4	3.1 ± 2.0
180 mins	10.5 ± 3.1	4.3 ± 2.6

RH, right hemisphere; LH, left hemisphere.

Table 3

Transient (15 mins) occlusion: group-average *M* and $CMRO_2$ from the primary forepaw somatosensory cortices (*n* = 8, mean ± s.d.)

	LH	RH
M (%)		
30 mins	9.2 ± 0.8	9.4 ± 0.4
90 mins	9.4 ± 0.6	8.6 ± 0.5
180 mins	8.2 ± 0.3	7.7 ± 0.4
24 h	8.8 ± 2.1	9.1 ± 1.6
$\Delta CMRO_2$ (%)		
30 mins	13 ± 3	13 ± 3
90 mins	19 ± 4	18 ± 3
180 mins	16 ± 3	17 ± 6
24 h	21 ± 10	23 ± 13

RH, right hemisphere; LH, left hemisphere.